All-in-one three-phase smart meter and power quality analyzer with extended IoT capabilities

Abstract

The traditional power grid is evolving into a new smart grid that requires better coordination of supply and demand, making it necessary to establish precise monitoring strategies in order to determine grid status in real-time. With the aim of providing a low-cost device based on open-hardware and open-source software to the technicians, engineers, and scientists around the world, this paper presents the three-phase openZmeter (3Ph-oZm), an all-in-one device that allows measuring and computing electrical data related to energy and power quality features in three-phase power networks. It has been designed to perform advanced computations for voltage, current, frequency, power, and energy. 3Ph-oZm is able to process high order harmonics, and log power quality disturbance events defined according to the recommendations of some international standards organizations. The data and its associated features are processed on-site using custom software specifically designed and programmed for this purpose that relies on advanced signal analysis techniques. This smart meter significantly improves the capabilities of the single-phase version, and overcomes certain shortcomings of other commercial devices, both in terms of versatility and data acquisition and processing capabilities. The system has been calibrated and validated using laboratory testing set-up and real-world applications, such as long-term photovoltaic power plant metering. The capabilities of 3Ph-oZm can also support a variety of other electrical applications, such as three-phase induction motor health monitoring, energy savings, or microgrid state estimation.

Keywords: Three phase smart meter, energy metering, power quality, Internet of Things.

1. Introduction

For decades, the extension of power grids has demanded the incorporation of advanced metering devices with remote capabilities such as smart meters, PMU or PQ analyzers to support the need for enhanced measurements. It is absolutely imperative to establish procedures that determine grid status to ensure a reliable transmission and distribution network [1].

The global trend in power systems is to be environmentally friendly and eco-resilient, with a clear circular orientation towards the exploitation of resources. Smart grids and microgrid systems allow the delivery of electricity in a controlled environment [2, 3]. Smart grids are built based on complex power models and decentralized electricity generation systems, thereby establishing a synergy between computer processing, control systems, and advanced renewable energy resources [4]. The management of smart grids requires accurately specifying their status in order to track and command them. This, in turn, requires the development of advanced measurement systems (smart sensors/meters). The 2012/27/EU directive [5] defines a *smart meter* as "an electronic system that can measure energy consumption, providing more information than a conventional meter, and can transmit and receive data using a form of electronic communication".

In addition to measuring power and energy, it is important to design high-precision devices to measure power quality (PQ), since the continuous incorporation of distributed generation systems based on renewable energy and non-linear loads in industry and home applications causes harmonics and PQ disturbances [6]. In particular, non-linear loads such as personal computers, fluorescent lamps with electronic ballast, and many other electronic components connected to the network may cause disturbances and deviations from the supplied voltage sinusoidal waveform. These current and voltage disturbances degrade and could damage modern devices [7, 8] and may impose penalties on consumers by adding reactive power, re-dispatch and load curtailment costs [9]. Power quality disturbances include sag/swell, outage, impulses, noise, imbalances, oscillatory transients, flicker and harmonic distortion, among others. The accurate detection and measurement of these disturbances has become a challenge for smart meter designers, who have proposed advanced signal processing techniques such as nonlinear optimization or nonlinear classification methods, including artificial neural networks and support vector machines [10]. Several researchers have proposed techniques for real-time detection and classification of power quality disturbances [11]. Improvement of communication and data processing techniques has allowed the integration of real-time detection events as functional blocks into smart sensors. These techniques include sophisticated and efficient algorithms [12, 13], such as Neural Network of General Regression for control strategies in microgrids with hybrid power supply sources [14]. The study of power quality often requires the application of signal processing techniques. The Discrete Fourier Transform (DFT) is the most widely used to date as it is often included in standards. Other methods that have become popular in recent years are the Short Time Fourier Transform (STFT) [15], Hilbert-Huang Transform (HHT), Stockwell Transform (ST) and Wavelet Transform (WT) [16, 17]. The features extracted by these advanced techniques are used to detect and classify [18, 19] the electrical events and PQ disturbances.

Given the current context, it is obvious that researchers, scientists, and professionals in the electricity sector still demand new high-precision and flexible devices for monitoring purposes. The information retrieved and processed by these meters can be used to improve the grid management and to solve issues related to security, including the verification of special conditions like ground fault current. This information will be valuable to implement corrective actions if necessary (e.g., using active or passive harmonic filters).

This study presents 3Ph-oZm, a low-cost three-phase smart metering and power quality analyzer with extended IoT capabilities. The manufacturing cost is currently below 100 USD. This innovation, derived from the single-phase openZmeter (oZm) [20], marks a major milestone. Its advanced design ensures a powerful, accurate, and reliable solution for power and electric energy metering in a wide range of operating conditions that aim to satisfy the specifications of IEC 61000-4-30 [21] and EN-50160 [22] for three phase meters. Bearing in mind the increasing number of devices that are currently required to monitor the power grid, this open-source device offers an efficient alternative to high-cost commercial meters.

1.1. Contributions and novelties

The main contributions and specific novelties of this paper are based on the following aspects:

- It is the first and unique three-phase system based on open software and hardware that can perform power, energy, voltage, current, frequency and power quality events measurements.
- Measurements in different configurations can be performed, such as three-phase three- or four-wire circuits, multiple independent single-phase loads or split two-phase systems.
- Raw data recording and streaming functionality is implemented in a general multi-purpose meter, so that it is possible to obtain the voltage and current samples in real time and at the maximum sampling frequency.
- All computation algorithms are fully open and can be audited by third parties. This functionality is not available in commercial devices.
- The system implements self-calibration capabilities based on heuristics. It also implements the capability of channel reordering by software without of rewiring cables.
- It is the first smart meter that implements the geometric algebra theory applied to electrical systems (see reference [23]).

Other interesting features not related to specific scientific contributions can also be listed:

- Thanks to its opensource philosophy, it implements an open API that provides all the computed variables according to standard interoperable protocols.

Table 1: New features and implementations in the 3Ph-oZm device compared to 1Ph-oZm developed in [20].

	1Ph-oZm	**3Ph-oZm**
System compatibility	Single phase	Three/single phase
Sampling frequency	16kHz	24 kHz
Electric tariffs management	NO	YES
Configurable alarms	NO	YES
ESIOS module	NO	YES
Self-Calibration module	NO	YES
Geometric Algebra module	NO	YES
Symmetrical Components	NO	YES
Voltage unbalance index	NO	YES
Harmonic power	NO	YES
MQTT protocol	NO	YES
Modbus protocol	NO	YES
Remote streaming & Cloud	NO	YES
External current probe	NO	YES

- For the first time, a powerful, customizable electrical tariff rate engine is integrated that can provide real-time electricity bill amounts based on the rate models of virtually any electricity company.
- It enables public energy price data to be obtained from other systems. Specifically, it is implemented to obtain energy and power prices from the Spanish ESIOS system.
- It is the only system that incorporates the computation of active and reactive power for the first 50 harmonics.
- A new module for alarms is implemented. It can be configured with generic expressions using a built-in formula engine generator.
- The computation of daily evolution of the first 50 harmonics of current and voltage is implemented.
- New protocols such as MQTT and MODBUS are also provided for compatibility with other devices.

The above features and novelties can be checked at the website project https://gitlab.com/zredalmeria/openZmeter.

1.2. Outline

The remainder of the paper is organized as follows: Section II describes the hardware design and software features of 3Ph-oZm; Section III presents the empirical validation of the device in different applications; Section IV provides the main conclusions obtained.

Table 2: Comparison of features among openzmeter and other comercial and opensource devices. Note: OPQ stands for Open Power Quality and OEM for Open Energy Monitor.

	3Ph-oZm	PQube3	Circutor MyEbox	Fluke 435	BMI HDPQ-DN	OPQ	OEM
Three phase capable	YES	YES	YES	YES	YES	NO	NO
Grid topologies	1ph/split/3ph	1ph/3ph	1ph/3ph	1ph/3ph	1ph/3ph	1ph	1ph
Open API	YES	NO	NO	NO	NO	YES	YES
Telegram notifications	YES	NO	NO	NO	NO	NO	NO
Configurable alarms	YES	YES	LIMITED	NO	LIMITED	YES	NO
Open Source	YES	NO	NO	NO	NO	YES	YES
Third party integration	YES	NO	NO	NO	NO	YES	YES
Open algorithms	YES	NO	NO	NO	NO	YES	YES
Waveform streaming	YES	ON EVENTS	ON EVENTS	ON EVENTS	ON EVENTS	ON EVENTS	NO
Tariffs and Billing	YES	NO	NO	NO	NO	NO	YES
Tariffs scripting language	YES	NO	NO	NO	NO	NO	NO
ESIOS integration	YES	NO	NO	NO	NO	NO	NO
Geometric Algebra processing	YES	NO	NO	NO	NO	NO	NO
Power harmonics	YES	YES	NO	YES	NO	NO	NO
Channel reordering	YES	NO	YES	YES	NO	N/A	N/A
Interface	WEB	LCD	LCD/ANDROID	Internal display	WINDOWS	WEB	WEB
Internal storage	8GB/CLOUD	32GB	16GB	8GB	4GB	CLOUD	CLOUD
Size	SMALL	SMALL	MEDIUM	MEDIUM	BIG	SMALL	SMALL
Manufacturing price	LOW	HIGH	MEDIUM	HIGH	HIGH	LOW	LOW

2. 3Ph-oZm description: Hardware and software design and implementation

3Ph-oZm has its origins in the single-phase device described in [20], which was designed as a reliable power and electrical energy meter primarily intended for use in urban or rural households. A major upgrade and extension of the original hardware platform has been designed, developed, and manufactured to be used in three-phase power networks, including advanced industrial applications. More specifically, without significantly increasing the dimensions of the single-phase version, 3Ph-oZm allows independent measurements to be carried out on each phase, that is, it is possible to measure different single-phase circuits at once. Furthermore, 3Ph-oZm admits a wide input current range as well as different types of probes, such as Hall sensors, Rogowski probes, or zero-flux probes to be used in three-phase power networks, mostly found in industrial environments. This feature enables a virtually unlimited current measurement capability (including DC). Another improvement is the incorporation of a internal Li-Po battery to enhance the device's autonomy. A list of the most relevant features included in the new device is listed in Table 1. Moreover, a comprehensive list of the novelties and capabilities compared to other existing comercial devices is presented in Table 2. As shown, it outperforms in a number of interesting features. Furthermore, none of the comercial devices available in the market implements all the specs and functionalities presented so far to the author's knowledge, thus the contribution of our work is clear as a potential all-in-one electrical meter for a wide set of applications.

The device has been specifically engineered to be a powerful tool for electrical measurements and to assist in power quality analysis applied to three-phase networks. Voltage and current waveforms are collected and analyzed according to the specifications of international standards EN 50160 and IEC 61000-4-30 (in some

Table 3: Details of main implementations defined in the Standards.

Feature	3Ph-oZm Implementation	Algorithm/Standard	Section
Time aggregation	10/12 cycle measurement. Aggregations for 150/180 cycles, 10 minutes, 1 hour	IEC 61000-4-30 – class A	4.4
Aggregation algorithm	150/180 cycle aggregation with resynchronization every 10 minutes aligned with UTC clock based on 10/12 cycles. 1 hour aggregation and additional aggregation of 1 minute y 15 minutes	IEC 61000-4-30 class A (Partially)	4.5
Time uncertainty	Continous NTP time synchronization	IEC 61000-4-30 – class A	4.6
Event flagging	All the values are tagged during events	IEC 61000-4-30	4.7
Frequency	Zero crossing method is used with filtering. A 3 second aggregation period is computed based on 150/180 cycles. The norm allows the use of periods shorter than 10s	IEC 61000-4-30/Custom	5.1
Voltage	RMS computation based on 10/12 cycles delimited by zero crossings.	IEC 61000-4-30 – class S	5.2
Sag & overvoltage	Half-cycle RMS measurements, based on zero crossings. The start, end and max/min values are recorded	IEC 61000-4-30 – class A	5.4/5.12
Interruptions	Half-cycle RMS measurements, based on zero crossings. The start, end and min values are recorded	IEC 61000-4-30 – class A	5.5
RVC	RMS measurements for half-cycle in steady state based on the standard recommendations. Events start once a deviation is detected. The event ends once the steady state is reached. Start, end and max. variation are recorded	IEC 61000-4-30 – class A	5.6/5.11
Unbalance	Symmetrical components for the voltage are computed and evaluated according to the standard	IEC 61000-4-30 – class A	5.7
Harmonics	Computed from 10/12 cycles using FFT (DFT). The first 50th harmonics are stored and aggregated	IEC 61000-4-30 – class B	5.8
Current	RMS computation based on 10/12 cycles delimited by zero crossings similar to Voltage. Harmonics computations similar to Voltage	IEC 61000-4-30 – class A	5.13

cases the class A design criterion has been implemented, as it is shown in Table 3). 3Ph-oZm is also a multipurpose IoT system since it can act as a power quality monitor, a smart meter, and an electrical event capable of communicating with other devices thanks to its advanced features (WiFi, Bluetooth, 3G/4G/5G, or Ethernet), which allow access to raw and computed data through the Internet. Typical HTTP web server and industrial communication protocols are specially implemented for industrial application, such as the Modbus protocol.

The sampling and conditioning signal stage is performed by a custom-designed Analog Front End (AFE) controlled by a realtime microprocessor-based system. The STM32F042 model, which belongs to the STM32 microcontroller family, was selected based on its high-end specifications, functionality, and low price. It is reliable and has high performance, real-time track signal processing capabilities, along with a low-power consumption combined with energy saving management. The current and voltage signals are sampled by means of a 12-bit Analog Digital Converter (ADC) with oversampling providing 13 effective bits. This ADC can sample signals at 24 kHz per channel, with a total of 7 channels (3 for voltage and 4 for current), encoding the digital data for streaming to the main microprocessor-based component, where the sampled current and voltage signals are preprocessed and conditioned by the STM32's digital signal processing (DSP) module. This preprocessed data is sent to a companion advanced RISC machine (ARM) board (mainboard), which executes the main process tasks. This mainboard ships with a custom compiled Real-Time (RT) Linux core OS (OpenWRT). It performs complex calculations such as Fast Fourier Transform (FFT), zero-crossing frequency estimation, or PQ event detection. The programmed C daemon service ensures the real-time strategy executing an endless loop with threads and queue management implemented.

2.1. Hardware design

In a general sense, electronic device-assisted PQ and/or smart meter systems are based on microprocessors or microcontrollers. Some of them are manufactured based on Field Programmable Gate Array (FPGA), while others use specialized electronic devices with specific modules like the Application-Specific Integrated Circuit (ASIC), which integrate most of the functions as a dedicated piece of hardware. 3Ph-oZm has been designed to maximize its flexibility, versatility, and minimize its cost. The hardware design and software features have been conceived to be both accessible and extensible as much as possible, leaving an open door to the implementation of new functions by adding new custom blocks. Advanced algorithms and specific analysis techniques can be implemented in a straightforward way. Based on the above principles, solutions in which most of the functionality is executed by specific hardware, such as FPGAs or ASICs, are discarded. Therefore, a minimal hardware is selected for acquisition and control, leaving complex and advanced tasks and computations for the RT Linux ARM multicore mainboard. This approach offers a minimal hardware setup for implementing all required basic features. Other complementary tasks like data storage and WEB services are also assumed by the RT Linux kernel. This embedded solution is very simple and efficient. Moreover, this combination of elements and parts also well suited to the concept of open-hardware and open-software. Figure 1 shows the block diagram of the 3Ph-oZm hardware where four conceptual blocks are clearly identified. The first block, in grey, contains the power supply and battery management. The input voltage is rectified from the mains side, converting Alternating Current (AC) to Direct Current (DC) up to 440 V in safety conditions. An analog pi filter is configured as a functional block to prevent noise sources. Rectified mains steps down by means of a buck converter Viper22A from STM Microelectronics, reducing the voltage to 22 V and offering up to 4.5 W. Finally, a secondary buck converter with the SY8201 chip, allows a stable voltage of 5 V. The use of this particular power supply allows the system to operate over a wider range of voltages than commercial integrated converters can tolerate, typically designed for the 100-240 V range. 3Ph-oZm has a Li-Po built-in battery for normal operation under blackout or abnormal voltage supply. This battery provides a voltage profile between 3.2 V and 4.2 V. All necessary electronics have been included to boost battery voltage to the board working voltage of 5 V (PS7516 module). The boost converter can be disabled by the microcontroller so that the whole system goes into sleep mode without damaging the battery by depletion. The charge process is also controlled while connected to the mains. The load manager chip is the TP4054 module, which limits the maximum charge current to about 100 mA. A dedicated metal–oxide–semiconductor field-effect transistor (MOSFET) element switches from mains to battery supply when the mains voltage is below 60 V. The second block accounts for the signal

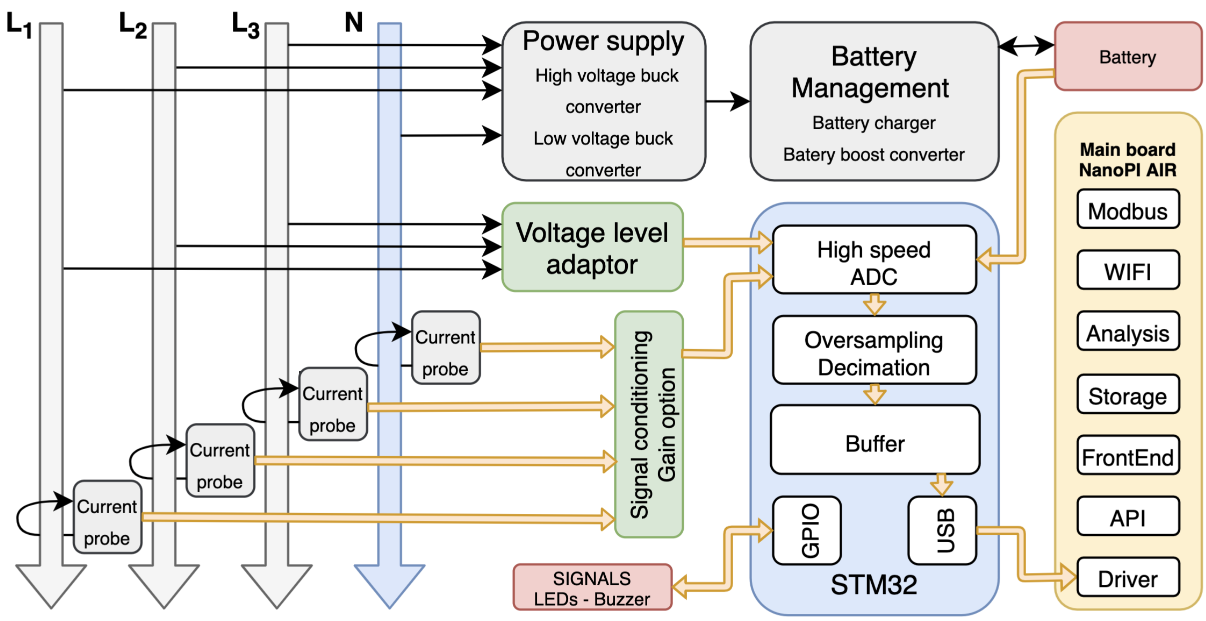

Figure 1: Three-phase openZmeter (3Ph-oZm) hardware block diagram: 1) the signal conditioning and acquisition (green); 2) the power supply and battery management elements (grey); 3) the STM32 microcontroller (blue), which controls the overall operation, performs data digitization and communication with the RT Linux kernel; 4) the Advanced RISC Machine (ARM) RT Linux board controller NanoPi (yellow).

acquisition part, which is highlighted in green. It contains the elements responsible for capturing the voltage and current waveform signals. For the voltage acquisition stage, a simple voltage divider is placed. It feeds an operational amplifier which also provides a low impedance signal to the ADC of the STM32. After the whole process, the input voltage range is reduced from ±440 V to 1.65 V±1.65 V, which is the suitable range tailored to the ADC's technical specification. The conditioning of every current channel is performed by using an operational amplifier MCP6004 from Microchip Technology, similar to voltage channels. The differential input signal is amplified and then adapted to a suitable input range of the ADC in the STM32 microchip. Moreover, the software-adjustable amplifier can be modified to control the output gain. This gain allows ±333 mV or ±625 mV values from the probes to be converted to the ±1.65 V input range of the ADC. For both voltage and current readings, the signal is filtered to eliminate high frequency noise. A high frequency passive low-pass anti-aliasing RC filter is configured to attenuate frequencies above 12 kHz, half the sampling frequency. The blue block is the STM32 microcontroller, which controls the overall operation, performs data digitization and communication with the Linux kernel using the USB channel. The system has been designed to operate at a high sampling rate. The voltage and current input values are sampled at high speed, along with the battery level and the internal voltage reference. The sampling

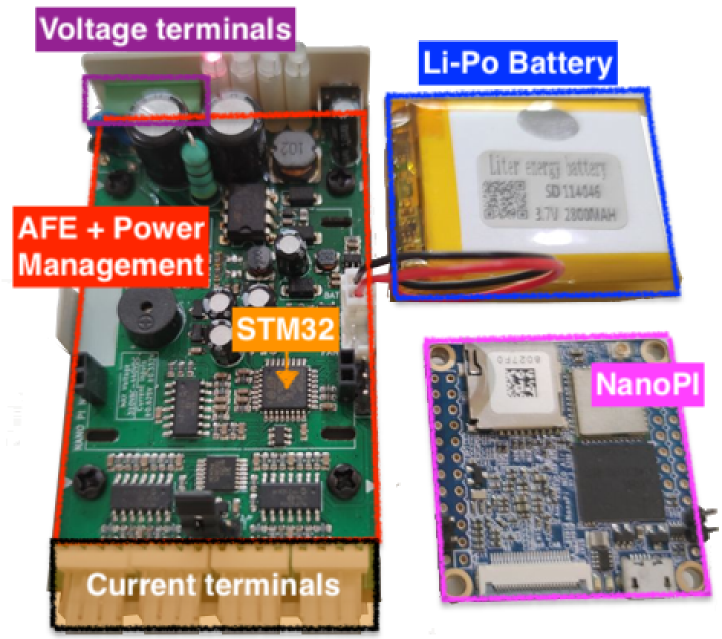

Figure 2: Main parts of 3Ph-oZm: Main board (left side), the Li-Po battery (top right) and the ARM Linux board controller (bottom right).

frequency is 96 kHz per channel, with 12-bit precision. Afterwards, a decimation process executed in the STM microcontroller allows resolution to increase, reducing the rate by 4. This yield a 24 kHz sampling frequency per channel with a 13 effective bit rate. The yellow block is the NanoPi Advanced RISC Machine (ARM) Linux board controller, which mainly analyzes, computes, stores and provides visualization services for the data obtained. It also provides a communication layer for WiFi and Bluetooth. Other technologies can be added by plugging USB peripherals, like an 3G/4G/5G USB modem, for example. All these blocks are integrated in a compact electronic device, with a typical width and height ratio for a DIN electrical device. The connectors for voltage terminals are located on the top side, whereas the terminals for the current probes can be found on the bottom side. The aforementioned terminals are mounted on the AFE board located immediately below the ARM mainboard (NanoPI). The Li-Po battery, WiFi antenna, and others auxiliary components are properly placed around the printed circuit board (PCB). Figure 2 shows the basic components of 3Ph-oZm. Note that the Li-Po battery, the heatsink, and other components are already included inside the enclosure. It can be seen that the main board design comprises the signal conditioning and acquisition stage, the power supply and management, the STM32 microcontroller and the interface to communicate with the ARM Linux board controller.

Voltage terminals are used for a dual purpose: to perform the measurements and to power the electronics

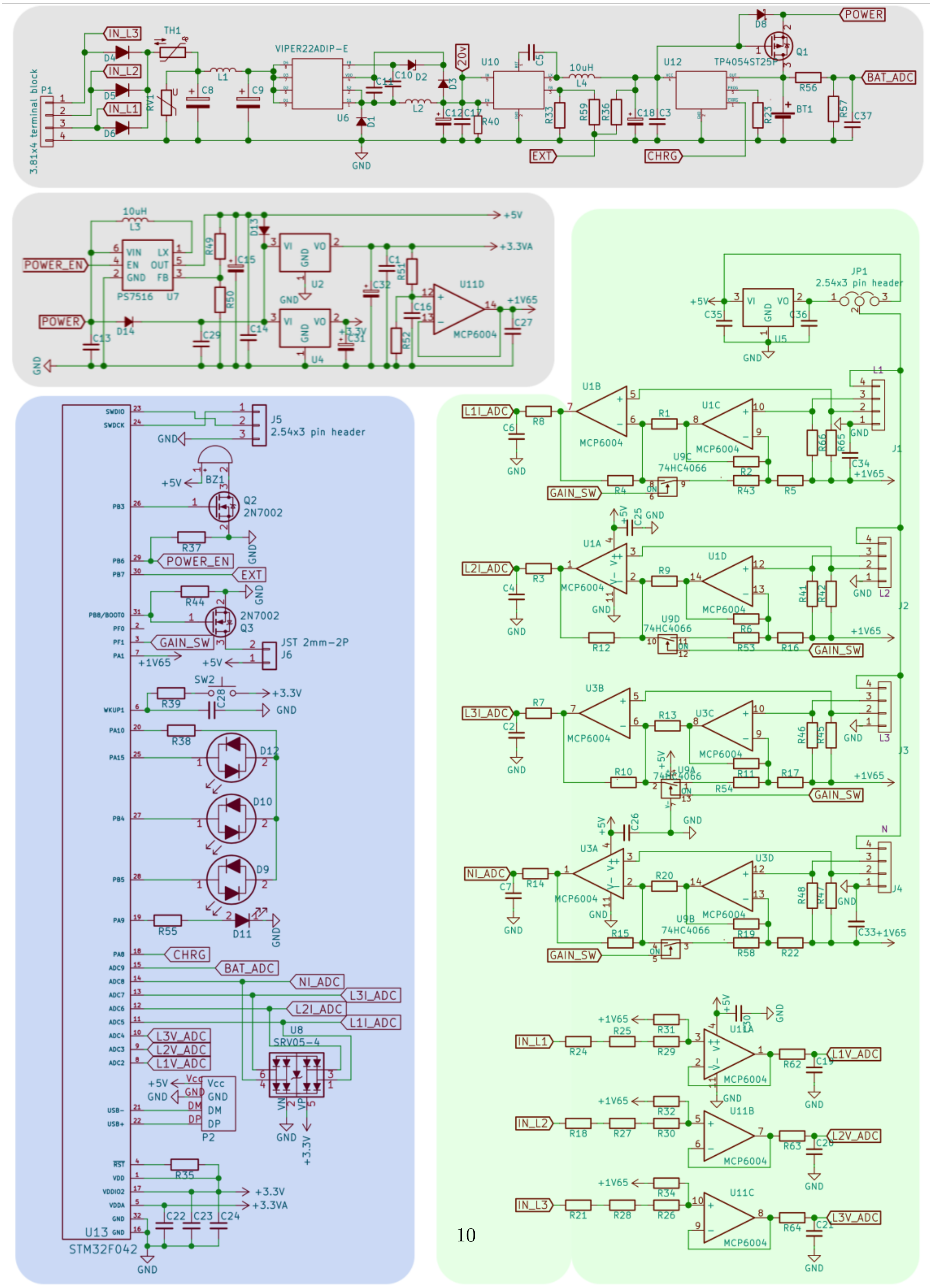

Figure 3: Electric scheme of the 3Ph-oZm. It is composed by the conditioning signal (green area), power management and power supply (grey areas) and the STM32 microcontroller (blue area). Note the connection to the ARM Linux board by pins USB+ and USB- in the STM area.

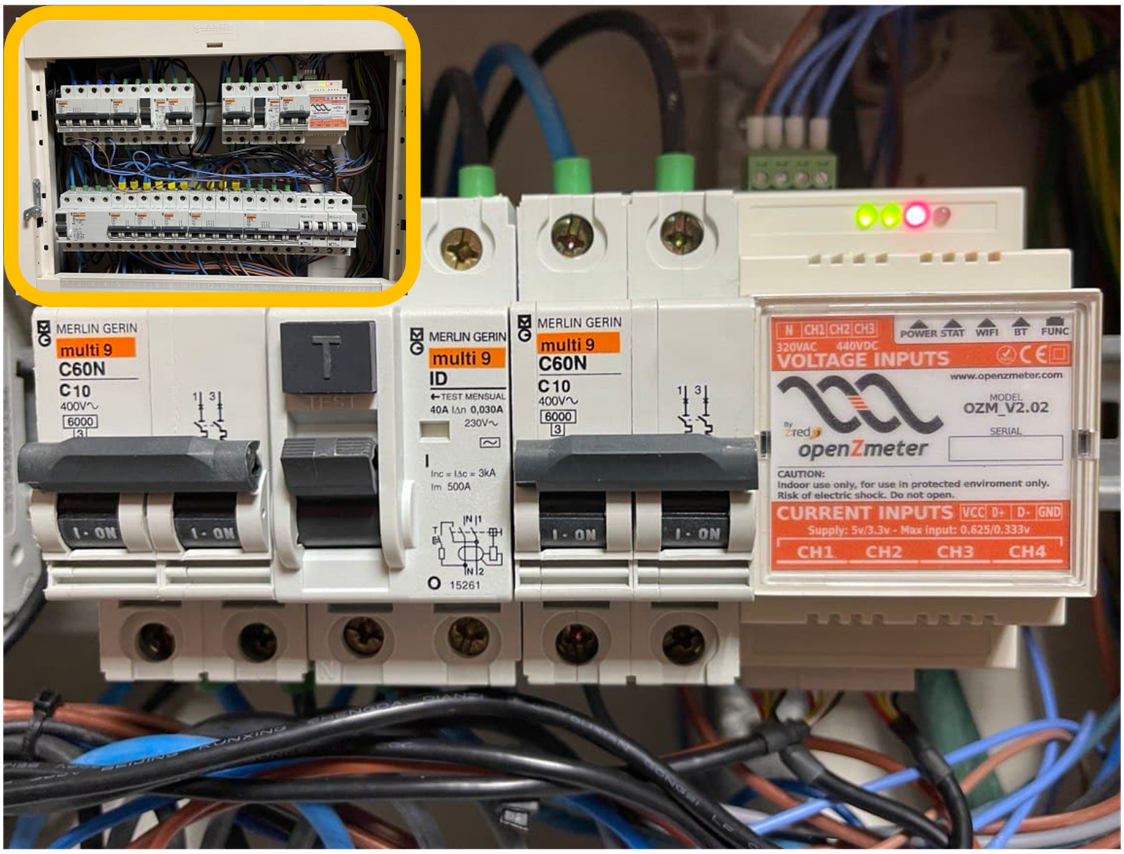

Figure 4: Electrical panel with a 3Ph-oZm installed along with circuit breakers and residual current breaker.

of the board. The power supply is not isolated from mains, which greatly simplifies the design due to the fact that all voltages are referenced to the neutral point. 3Ph-oZm is completely functional even if only one phase is active (used for the power supply), so it can also be used in single-phase and two-phase systems. Every line current can be measured separately, including the neutral. It allows different configurations to adapt to different measurement probes. The probes can be configured for two voltage supply levels (3.3 V and 5 V). The operating mode is performed by changing the position of a jumper, which must be provided with the appropriate connection. The input voltage range of the current probe can be adjusted to ±333 mV or ±625 mV by software control, which is a typical differential input. The current channels can be configured for different types of probes. Among the probes that can be connected to the device are:

- *Current transformers*, a type of passive probe that requires no power supply. They are very low-cost and widely used in many measuring devices. Their accuracy is acceptable with a significant phase variation.
- *Hall effect sensors* are active probes requiring external power supply. They have good accuracy and phase response. These sensors typically operate at 5 V and have an output of 2.5±0.625 V.
- *Rogowski probes*, admit high currents for specific applications in large electrical installations. The set-up is accomplished by clamping to the busbars. Most of them have an output of ±333 mV at 1000 A. They are typically supplied at 5 V and have high accuracy and very good phase response.

Figure 3 shows the designed scheme of the manufactured electronic device. The scheme and silkscreen of the PCB has been created using the cross-platform Kicad [24], an open source electronics design automation suite.

As it can be seen in Figure 4, the installation of 3Ph-oZm in a real electric cabinet is very straightforward since it has been designed to be attached directly to the DIN rail. Voltage wires need to be connected to the terminal block. The current probes can be installed on each phase wire without altering the installation.

2.2. Software design

The description of the software design of 3Ph-oZm is divided into two parts: daemon services and web front-end.

2.2.1. Daemon services

The software runs in an endless loop programmed through daemon services, which are executed automatically at startup. The embedded ARM unit is in charge of executing the code by means of a real-time kernel (Linux RT). It ships a wireless module (AMPAK AP6212) with WiFi 802.11b/g/n and Bluetooth 4.0 dual mode, ready for Internet applications. The daemon software is coded using C++ to achieve a robust and reliable service. To make the service as extensible as possible, two distinct blocks have been defined within the service: The first one is the capture driver, that is responsible for reading the raw samples as well as making the necessary adjustments and passing them to the second block (the analyzer). This analyzer is responsible for processing the samples, storing them, and serving the results to the clients. The driver feeds one or several analyzer blocks, each one working independently on the input sample stream and generating results on the injected channels.

Figure 5 summarizes the analysis process consisting of data input through the USB port of STM32 microcontroller until results are obtained and stored. The first block, in blue, corresponds to the reading of the data generated by the STM32 microcontroller. Since it has a very small amount of internal memory, the reading from the USB port must be continuous and without interruptions for more than a few milliseconds. After receiving the data, the configured calibration settings are applied to translate the value obtained by the ADCs to the corresponding voltage and current, labeling the samples with the timestamp corresponding to the instant of reading. This time stamp is accurately preserved by using a network time synchronization service. The channel rearrangement is the final stage. Here, the channels used, their polarity and the order of the different available analysis modes can be selected. Note that the measurement of several independent single-phase systems can be accomplished. It also allows fix errors in the wiring connection. The order of the phases can be rearranged without the need to modify the physical connections.

As the data input flow is continuous and the time required for the analysis process and data storage may varies depending on the system load or connected clients, the first step of the analysis is the storage and segmentation of the samples into blocks. The zero crossing block takes the input voltage waveform and passes it through a bandpass filter. A five-stage biquadratic (2-poles and 2-zeros) digital filter is used. The required filter coefficients are calculated at the start of the capture process so that the nominal frequency can be conveniently detected (defined in settings), and the zero crossing detector can count the number of cycles properly. The phase shift introduced by the filter needs to be compensated, adding the same delay to the rest of the channels. Using the recommendations of IEC61000-4-30, the preferred time interval for the voltage waveform is 200 ms, which means 10 cycles for 50 Hz systems and 12 cycles for 60 Hz systems. Therefore, a 200 ms data package is used to compute all subsequent parameters and features.

The ARM board has a 4-core CPU so it has a high concurrent processing capacity. Thus, for each basic block of 200 ms and channel, the Root Mean Square (RMS) values of voltage and current are calculated.

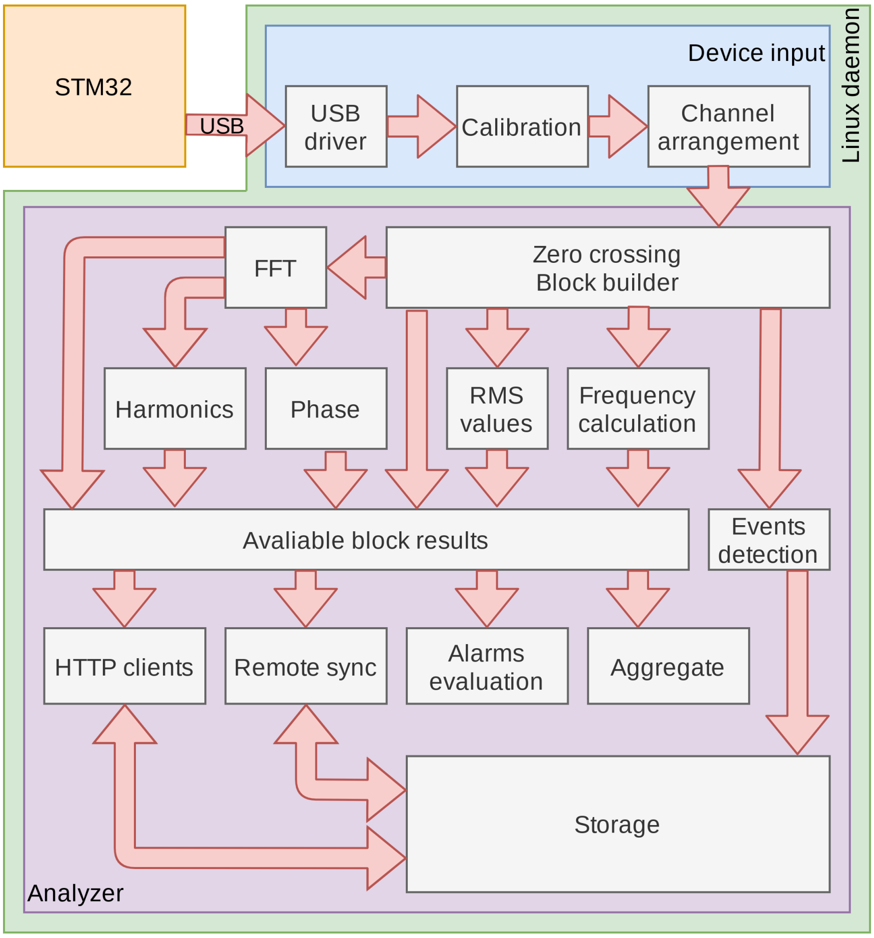

Figure 5: 3Ph-oZm Linux daemon blocks, driver capture in blue, analysis stages in purple

Moreover, an FFT is initiated using a stable well-known open-source implementation (FFTW3) [25] so that harmonic voltage and current are also computed. For the real grid frequency, the length of each half-cycle during the last 10 seconds is taken into account. Once the FFT is completed, further calculated parameters can be obtained: active, reactive, and apparent power, power factor, harmonics up to 50th for current and voltage, phase shift between current and voltage, active and reactive energy, symmetrical components and unbalance factor. The event detection process runs in a separate thread since an event can span several 200 ms blocks. If an event starts or is running in the current block, the start and end samples are stored (both waveform and RMS voltage values) and the block and subsequent aggregations are marked as affected.

The results produced after the analysis of each block can be consulted in real time, including the waveforms of each channel and the spectrum obtained by the FFT in the frequency domain. However, following IEC61000-4-30, the data obtained are aggregated in larger time blocks of 3 seconds, 1 minute, 10 minutes, 15 minutes and 1 hour. The data are stored into a local database and it is possible to retrieve aggregated data using custom methods implemented in the software. Furthermore, all captured data can be retrieved through an API Rest, with the possibility of synchronization with cloud services through the MQTT protocol. This enables real-time data provided by multiple devices to be available at a central location.

2.2.2. Web frontend

All the information generated by 3Ph-oZm is stored locally in a PostgreSQL database and can be queried through a series of functions defined in a Rest API. However, one of the main tools provided is the visualization and monitoring application, accessible through the web portal embedded in the device itself. All measured data are served in real time, refreshed dynamically using leading-edge web technologies such as HTML5, CSS3, and Javascript. Different graphs are synchronized to display information for the same time span. The web application is mainly organized into three sections: Analysis, Events and Energy stats. It also includes a general dashboard view with the main variables and other menus for the configuration of the device. The main drashboard of the application is shown in Figure 6, which displays the most relevant features and parameters of the electrical system. The application layout is distributed as follows: top right, brief overview for RMS voltage, RMS current, active power, frequency, and energy; middle, last 2 hours evolution for RMS voltage, RMS current, active power and frequency; bottom, last 24 hours evolution for several important features; left, sidebar to access all menus.

Regarding the PQ disturbances, 3Ph-oZm features three tools for management, visualization and analysis. The first tool is based on the international standards IEC 61000-4-30 and EN-50160, and includes the event counting and statistical distribution of frequency, mains voltage, total harmonic distortion (THD),

Figure 6: Application screen display of 3Ph-oZm. Top right shows the main hardware parameters summary. In the top left, the main status parameters are displayed, such as battery charge, WiFi connectivity and data storage level. On the left, 3Ph-oZm offers different options. The main screen area displays the detailed measurements, namely voltage, current, active power and frequency.

and unbalance. The second tool is the event manager, which is based on the recommendations provided by the Information Technology Industry Council (ITIC) and Computer Business Equipment Manufacturers Association (CBEMA) and allows visualizing the distribution of recorded grid events, such as rapid voltage changes, voltage gaps, among others.

2.2.3. *Calculation of electricity prices*

In addition to acquiring and processing power consumption and power quality data in real time, 3Ph-oZm allows the determination of the cost of the energy consumed. In the case of Spain, the grid energy cost for regulated rates is published daily on ESIOS (https://www.esios.ree.es/en/pvpc), the platform of Red Eléctrica de España (the Spanish electricity system operator).

From June 2021, domestic users contract the new 2.0TD tariff, corresponding to power ratings up to 15 kW. This is a tariff with hourly discrimination that has three consumption periods (valley, flat and peak) and two power periods (valley and peak). Therefore, ESIOS provides an API to get the hourly price of electricity, such that 3Ph-oZm access to data provided by ESIOS while also allowing to define parameters of the contracted tariff, including the periods, the contracted power (in kW), etc.

Figure 7 shows how 3Ph-oZm is able to define the periods and variables to be analyzed according to the contracted electricity tariff, as well as the visualization of the energy cost in different time periods, which allows an efficient management of these costs, a critical aspect in industrial facilities with high electricity consumption.

3. Experimental results

Testing and calibration procedure were executed at the electrical engineering laboratories of the University of Almería (Spain). All data were recorded and stored locally in the 3Ph-oZm, but they were also publicly available using the WiFi network of the university (it is also possible to send the data to a server or cloud using a 4G/5G USB modem). The setup requires installing the 3Ph-oZm in the DIN rail of an electrical panel, as Figure 4 shows. The calibration set-up is shown in Figure 8, which includes a three-phase variable voltage source (model DL 1013T1, manufactured by the De Lorenzo Group), with input voltage from the mains and output voltage through auto-transformer adjusted by means of a rotary knob, two high-accuracy 8.5 digit reference multimeters (Fluke 8558A) with maximum resolution of 1 nV and maximum deviation 4.0 μV/V with confidence interval at 95% and 5.7 μV/V confidence interval at 99% and a programmable single-phase power supply (Agilent model 6812) which has a maximum harmonic distortion

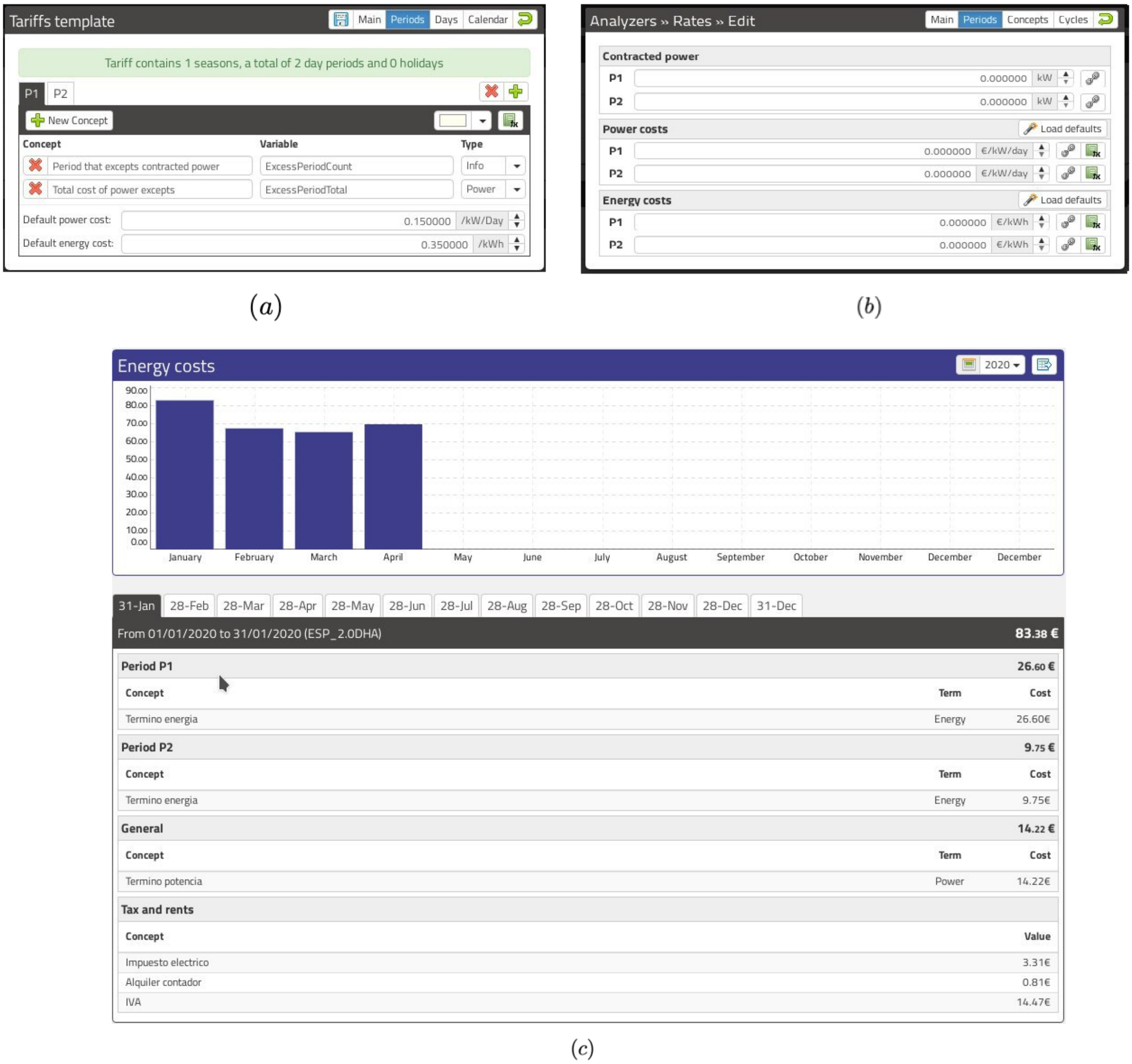

Figure 7: (a) Tariff template; (b) Customized information; (c) Energy costs of the energy consumed.

Table 4: Operating scenarios considered in the empirical study.

Case	V_{RMS} (V)	Description
1	143	Phase T with parallel RC load (R is moved from position 0 to 7 for 1 second; L in position 7 all time).
2	143	Phase T with parallel RL load (R moved from position 0 to 7 for 1 second; L in position 7 all time).
3	220	Phase T with parallel RL load (R moved from position 6 to 7 for 1 second; L in position 7 all time).
4	220	Phase S and T connected to inverter. Phase T with parallel RL load (R moved from position 0 to 7 for 1 second; L position 2 all time).
5	220	Phase T with parallel RL load (R moved from position 3 to 4 for 1 second; L in position 4 all time).

of 0.25% with 0.5% load regulation and an output voltage error of 0.15% between 45 and 100 Hz. The calibration procedure consists of a series of specific steps. First, a custom voltage is generated and applied to a linear load for about 5 minutes. During this period, raw readings of the generated waveform for each of the channels (voltage and current) are recorded with the 3Ph-oZm and the precision multimeters. The instantaneous synchronization function of the multimeters is used to ensure that these readings are taken at the same instant. Subsequently, the RMS voltage and current values are calculated in the multimeters as well as in 3Ph-oZm, applying the necessary gain and offset corrections (both adjustments are made by software). After this step, the consumed active power is computed, and the phase correction values are applied. Phase correction, which is applied in all the available channels, is necessary for accurate active and reactive power readings, especially since each type of current sensor may require different values to compensate for the phase shifts introduced by construction.

In order to verify the calibration process, the voltage and current harmonic values obtained by 3Ph-oZm where compared with the equivalent measurements provided by a Fluke 8558A analyzer as a reference standard, under sinusoidal conditions at a frequency of 50 Hz, where the Fluke analyzer presents its best performance and very high accuracy. The methodology to be used to determine the quality of the measurements will follow the pattern of other recent studies on new smart meters in which different operating scenarios are analysed [26].

The operating scenarios here analyzed are described in Table 4. They are based on the use of inductive

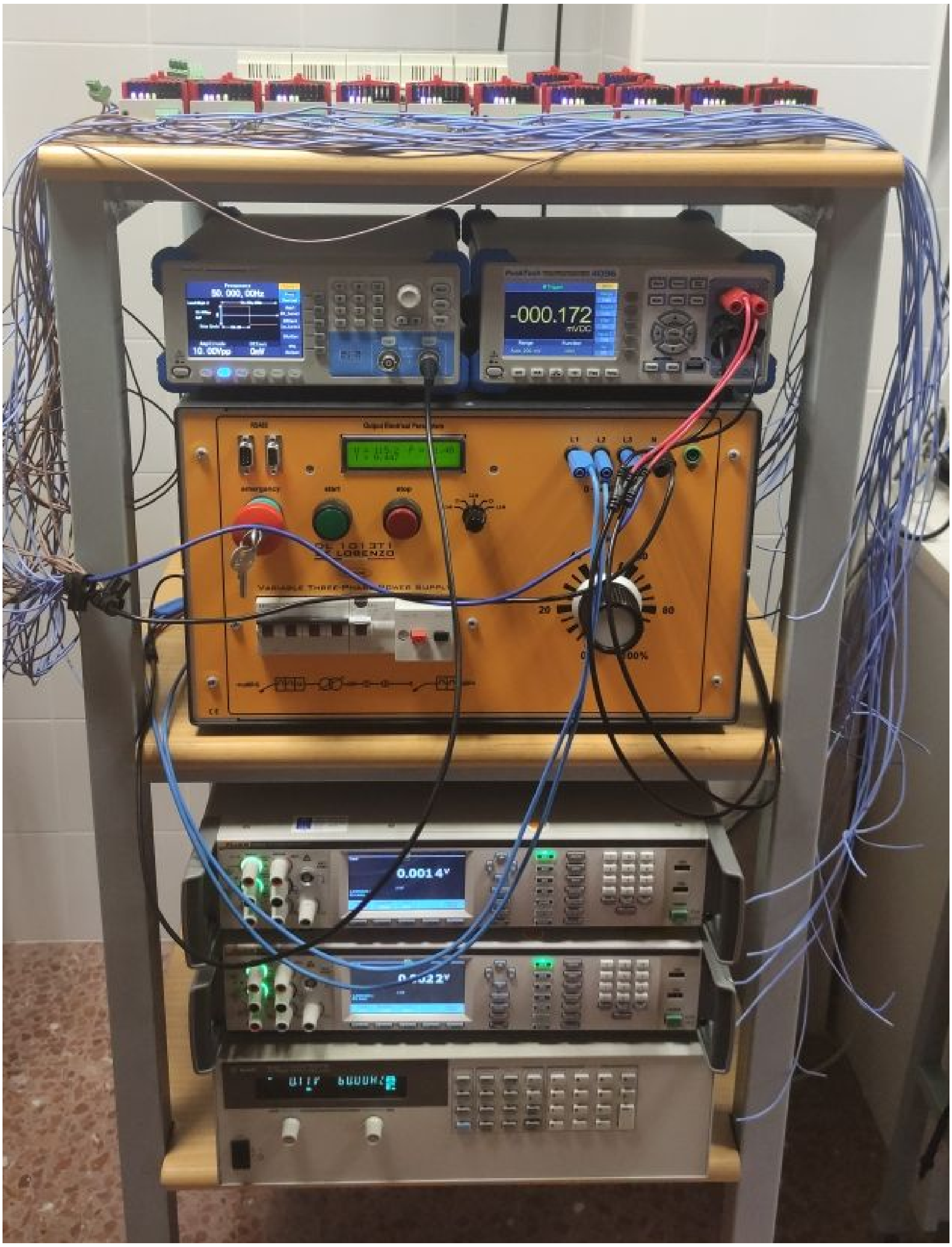

Figure 8: Equipment used to calibrate 3Ph-oZm: On top, some 3Ph-oZm's prepared to be calibrated. DL 1013T variable three-phase power supply is shown in yellow box, while two 8.5 digit high accuracy multimeters Fluke 8558A and an Agilent 6812 digital power supply are located at the bottom.

Table 5: Comparison between the measurements of 3Ph-oZm and Fluke 8558A considering the five first voltage and current harmonics.

	Device	Min	Max	Mean	SD	Skewness	Kurtosis
Experiment #1							
V	3Ph-oZm	139.511	143.070	141.599	0.961	-0.388	-0.323
	Fluke	140.177	144.433	142.603	1.236	-0.208	-0.958
I	3Ph-oZm	0.774	1.373	0.860	0.175	2.786	6.605
	Fluke	0.776	1.375	0.866	0.174	2.790	6.628
Experiment #2							
V	3Ph-oZm	139.256	142.541	140.876	1.005	-0.118	-1.009
	Fluke	139.710	143.559	141.489	1.163	-0.059	-0.791
I	3Ph-oZm	0.742	1.374	0.875	0.234	1.585	0.915
	Fluke	0.748	1.375	0.881	0.231	1.591	0.937
Experiment #3							
V	3Ph-oZm	217.810	220.510	219.698	0.745	-1.301	0.857
	Fluke	218.090	220.981	220.063	0.814	-1.161	0.449
I	3Ph-oZm	0.391	1.442	0.497	0.108	2.887	7.038
	Fluke	0.397	1.422	0.492	0.315	2.888	7.038
Experiment #4							
V	3Ph-oZm	217.610	220.310	219.498	0.715	-1.276	0.812
	Fluke	218.095	220.983	220.062	0.814	-1.159	0.445
I	3Ph-oZm	0.383	1.340	0.422	0.102	2.485	6.991
	Fluke	0.388	1.325	0.452	0.215	2.666	7.247
Experiment #5							
V	3Ph-oZm	219.510	220.050	219.764	0.140	-0.079	-0.329
	Fluke	220.077	220.571	220.272	0.140	0.317	-0.214
I	3Ph-oZm	0.710	0.911	0.744	0.063	2.059	2.645
	Fluke	0.697	0.915	0.765	0.064	1.877	2.261

(DL 1017L), capacitive (DL 1017C), and resistive (DL 1017R) loads manufactured by De Lorenzo [27]. They are controlled by switches with seven steps (positions) each. Phases R, S and T are connected to the three-phase variable source in all the scenarios, but the channels are configured in different ways, as it is described in Table 4.

The 3Ph-oZm device is reasonably accurate. For voltage measurements (considering all harmonics), the 3Ph-oZm has an average accuracy of 99.9% with a standard deviation of 0.16 V. The voltage with a 95% of confidence interval fluctuates by 0.4% with respect the mean value. The confidence interval fluctuation is calculated as the difference between the upper and lower bound voltage and divided by the mean value. This yields a voltage uncertainty of 0.094% using the standard definition of measurement uncertainty. For the current case, and considering all harmonics, 3Ph-oZm has an average accuracy of 91.178% with a standard deviation of 0.05 A. The current with a 95% of confidence interval fluctuates by 1.9% with respect to the mean value. This results in a current uncertainty of 0.822% using the standard definition of measurement uncertainty.

A series of experiments have been designed consisting of measuring the voltage and current of a load for one second. All experiments have been performed in the same way. The data set obtained consists of a series of RMS voltage and RMS current values. Therefore, a maximum value, a minimum value and an average value can be calculated. In addition, it is possible to calculate the standard deviation and other statistical numbers such as skewness and kurtosis. Each statistical number analyses the location and variability of the data set. The skewness is a measure of symmetry of the data set distribution and kurtosis provides the trend of the data set to give a set of outliers.

Table 5 presents the average statistical measurements of the five scenarios presented in Table 4 for the 3Ph-oZmare and the high-accuracy 8.5-digit reference multimeter (Fluke 8558A) when measuring voltage and current fundamental harmonic. The standard deviation (SD) is less than 1 V. The experiments are carried out using two different voltages, 143 V and 220 V respectively. The statistical asymmetry for voltage is very low giving centered values for this measurement. On the other side, the one for current is slightly positively positioned, as expected, due to the sequential increase of the resistance in the successive experiments. All values for Shapiro–Wilk normality test were far above for the chosen significance level (0.05). Therefore, we do not reject the null hypothesis. Parametric tests were performed because all variables followed a normal distribution. Figure 9 shows the normal Q-Q and detrended normal Q-Q plot for both 3Ph-oZm and Fluke devices, considering the first voltage harmonic. The data performance is similar for 3Ph-oZm and Fluke; being the trend equivalent in the context of a data representation as normal distribution. The magnitude

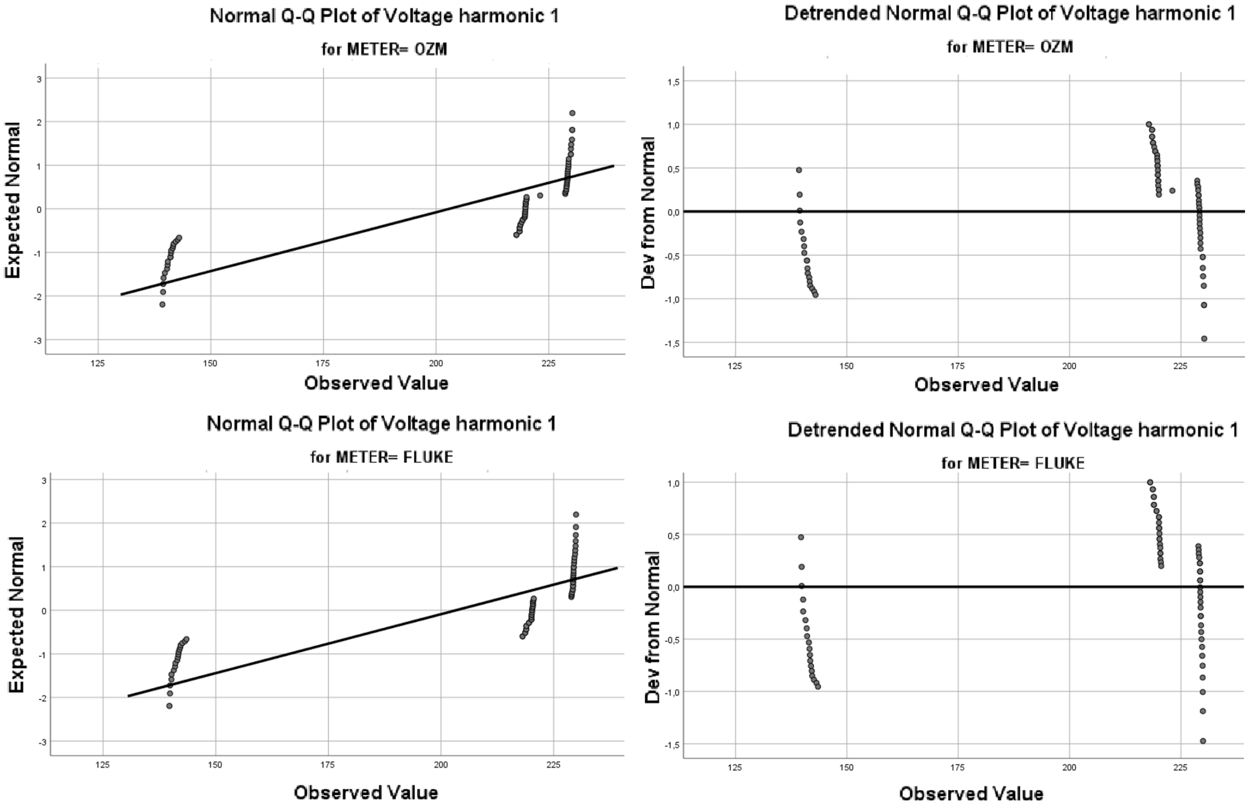

Figure 9: Normal Q-Q plot (left column) and Detrended Normal Q-Q plot (rigth column) of 3Ph-oZm (top row) and Fluke 8558A (bottom row) considering the first voltage harmonic.

and direction of deviation in the observed quantiles in the Gaussian model match each other. Therefore, there is no statistical difference, validating the measurements made with 3Ph-oZm and Fluke in the same conditions.

An analysis of variance (ANOVA) with a 200 × 50 (50 harmonics calculated using FFT) was carried out for the 3Ph-oZm and high-accuracy 8.5-digit reference multimeter (Fluke 8558A) to determine differences in the current and voltage measurements. Table 6 shows the result for the first three harmonics. The numeric columns represent (from left to right) the quadratic sum of experimental values $\left(\sum x_i^2\right)$, the degree of freedom (df), the quadratic mean ($\bar{x}^2$), the F value in statistics (F), and the p value in statistics (p). The Mauchly's sphericity test applied to the ANOVA results was performed to assess the assumptions of variance. The type I error of measurement (false positive) was reduced using the Greenhouse-Geisser method for the correction of the freedom degrees in order to obtain sphericity assumptions. Statistical calculations were performed using the IBM SPSS software v.26. The significance level used here is 0.05 ($p < 0.05$). As it can be observed, values higher than 0.05 are obtained, which involves the non-independence of the two

Table 6: Analysis of variance for 3Ph-oZm and Fluke 8558a.

		$\sum x_i^2$	df	$\bar{x}^2$	F	p
V_1	Between Groups	5.015	1	5.015	0.004	0.952
	Within Groups	188,910.361	138	1368.916		
	Total	188,915.376	139			
I_1	Between Groups	0.000	1	0.000	0.001	0.979
	Within Groups	32.728	138	0.237		
	Total	32.728	139			
V_2	Between Groups	0.016	1	0.016	0.045	0.832
	Within Groups	47.978	138	0.348		
	Total	47.993	139			
I_2	Between Groups	0.000	1	0.000	0.087	0.769
	Within Groups	0.025	138	0.000		
	Total	0.025	139			
V_3	Between Groups	37.140	1	37.140	42.646	0.977
	Within Groups	120.185	138	0.871		
	Total	157.325	139			
I_3	Between Groups	0.000	1	0.000	0.005	0.942
	Within Groups	1.399	138	0.010		
	Total	1.399	139			
Angle	Between Groups	0.381	1	0.381	0.000	0.994
	Within Groups	1,048,872.624	138	7600.526		
	Total	1,048,873.006	139			

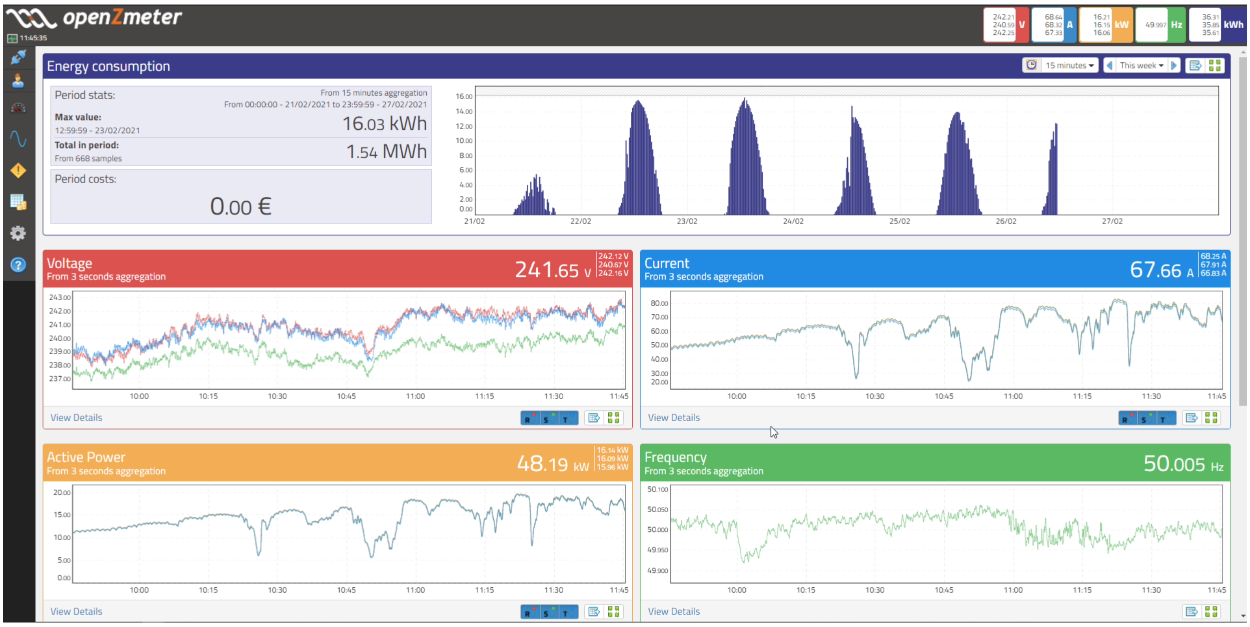

Figure 10: Main dashboard for a real 100kW PV power plant located in Almeria (Spain). This view displays the energy generated and the main RMS values.

variables compared (voltage and current).

4. Operation of 3Ph-oZm in real environments: The case of a PV power plant

This section describes the use of 3Ph-oZm in real-world applications. More specifically, the information here presented corresponds to the measurements taken in a 100 kW photovoltaic (PV) power plant located in Almeria (Spain). Figure 10 shows the main dashboard for the PV power plant. The daily energy cycle for a period of one week can be observed. As expected, the energy cycle exactly matches the sun's cycle from sunrise to sunset.

The device performed satisfactorily and it was possible to perform the monitoring and PQ analysis remotely on a central location using a modern browser:

- Voltage Analysis: The voltage and its RMS value are measured in real time. The measurement are presented for both instantaneous value and the wave form. The visualization of the waveform is conducted every 10 cycles. Moreover, this voltage view (see Figure 11) has advanced options, such as harmonic visualization, FFT visualization, complex phasors representation, among others.

- Current Analysis: The current waveform is measured in real time for all three phases. The raw samples and RMS value are presented in several web views. The waveform visualization is retrieved every 10

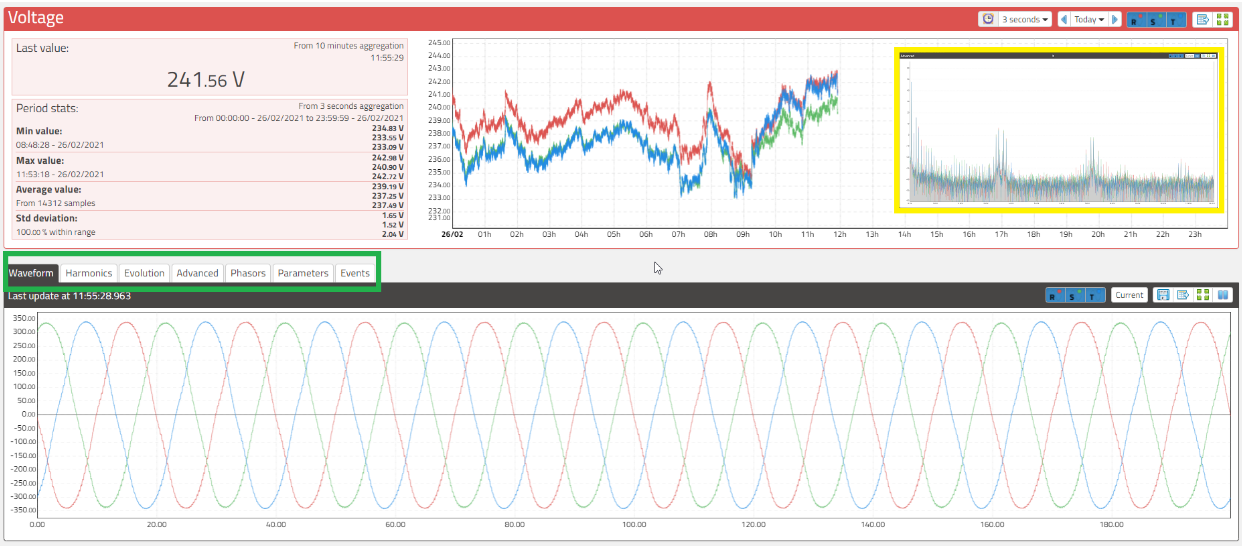

Figure 11: Voltage view for the 3 phases measured. The view shows the RMS for each phase and the voltage waveform. The green rectangle shows the different options available in the this view. The yellow rectangle shows the advanced option where it is possible to observe the three-phase FFT.

cycles. In addition, the Current web view (see Figure 12) has advanced options that can be selected using the tab control green rectangle, including the phasor view (Figure 13), harmonic visualization, or FFT visualization, among others.

- PQ Analysis: Custom algorithms have been developed to monitor swells, dips, interruptions, and rapid voltage changes considering the standards IEC61000-4-30 and EN-50160. The layout for PQ disturbance visualization was organized using three views. The first view is the ITIC/CBEMA curve, where a permitted zone, prohibited zone, and no-damage zone are defined. Every disturbance is presented by registering the magnitude of voltage RMS value and time duration. There are some charts that show the statistics computed from these events. The second view is a timetable where each recorded event is presented, while another table is used to select and visualize the waveform during the event (several cycles before and after). In this way, it is easy to observe what happened before and after the normal restoration of the voltage. The last view (see Figure 14) displays a visualization and statistics of the different types of events.
- Active and reactive energy stats: These measurements are carried out using a time interval, which allows to easily calculate the accumulated energy values. It is possible to visualize the energy grid data in order to analyze the energy consumption habits and, alternatively, use a energy heat map where each colored "pixel" shows the consumption made in a specific time interval. In Figure 15

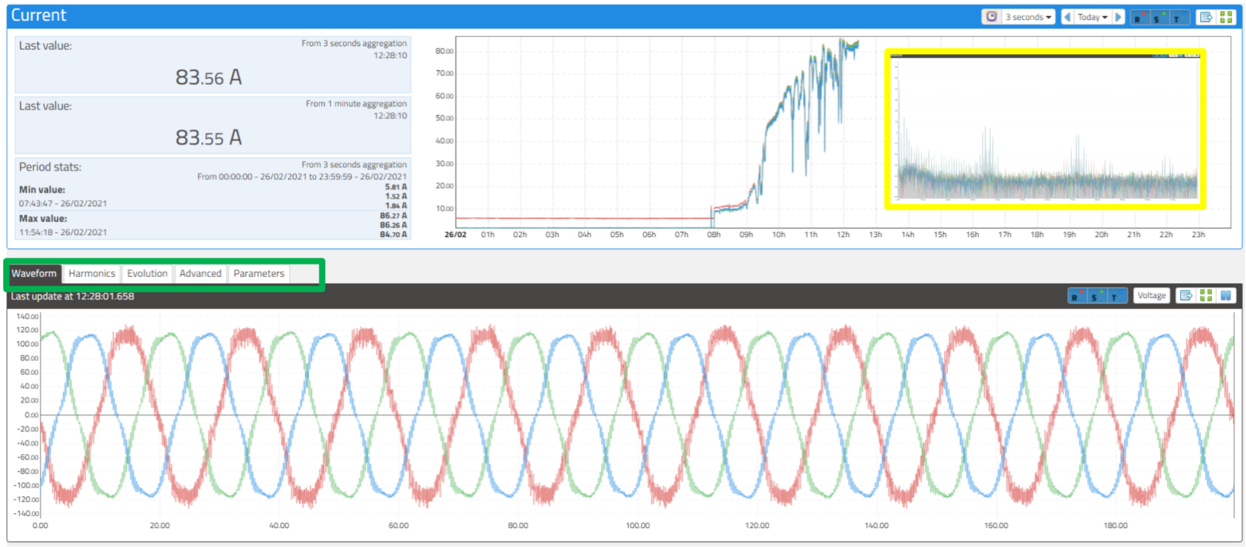

Figure 12: Current view for the three phases measured. The view shows the RMS for each phase and the current waveform. The green rectangle shows the different options available in the this view. The yellow rectangle shows the advanced option where it is possible to observe the 3 phase FFT.

the heatmap of a power plant is shown. In this case the colormap represents generated (instead of consumed) energy. The user can select the colormap by software in the configuration tab depending on the functionality or custom needs.

5. Conclusions

This paper presents 3Ph-oZm, an all-in-one three-phase smart meter and power quality analyzer with advanced IoT capabilities intended for industrial applications in large electric facilities. This device is based on open-hardware and open-source principle. It has been been designed to have an high accuracy while satisfying several international standards such as EN 50160 and IEC 61000-4-30. It is able to acquire and process large volume of data with low power consumption, while displaying a large number of electrical parameters using modern visualization methods. The device has been calibrated using ultra-high precision reference multimeters. Several laboratory tests and a real case in PV power plant have shown that it is a precise and high-quality multipurpose smart meter. The 3Ph-oZm smart analyzer is very versatile, since it includes functions for monitoring multiple energy consumption and power quality variables, which allow it to be used in any real environment.

The main innovation of the project is the creation of an autonomous, small-size and low-cost device that is able to process electrical and energy data along with power quality events in three-phase electrical grids.

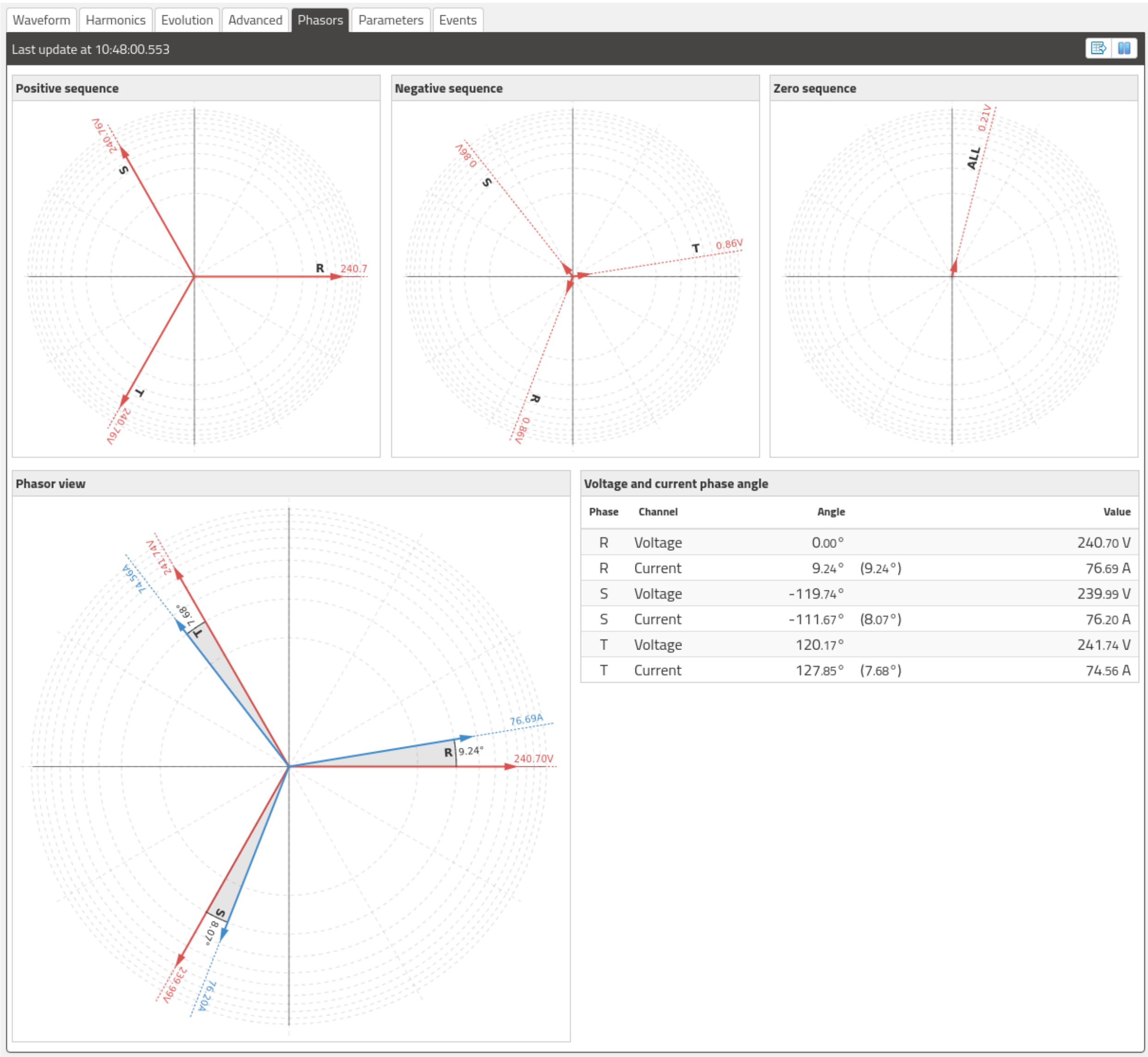

Figure 13: Phasor view for the three phase system. Symmetrical components are shown at the top and the complex phasor representation at the bottom.

Figure 14: Statistics based on standard EN-50160.

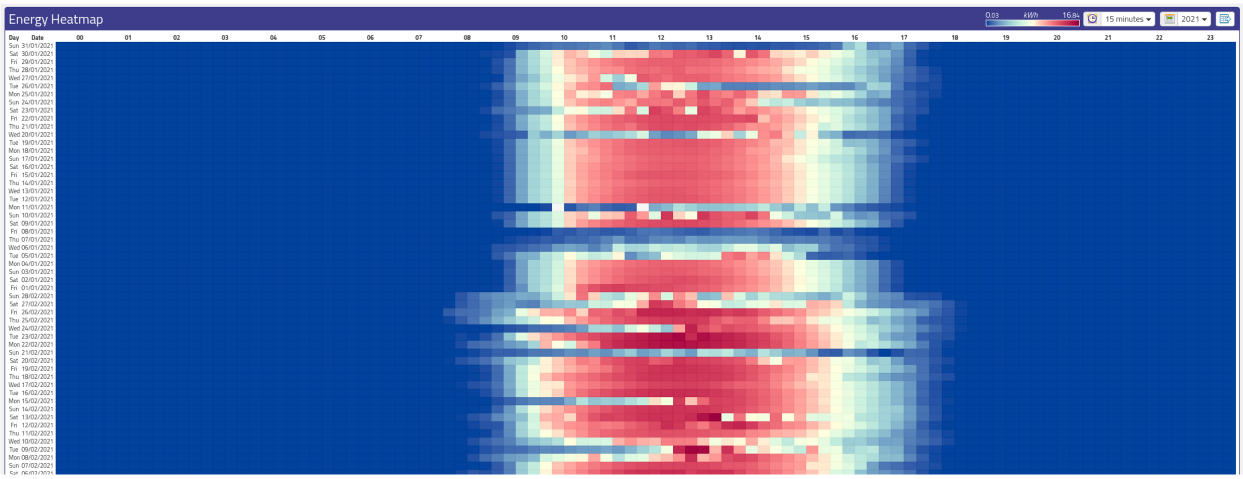

Figure 15: Active energy heatmap processed by 3Ph-oZm in a 100kW PV power plant located in Almería (Spain). Red colors indicate higher values for generated energy.

It is designed not only as a stand-alone device that can process the collected information on-site, but also as an IoT endpoint that syncs the information with the cloud. With regard to adaptability and the ability to acquire and process data, the 3Ph-oZm greatly enhances the capabilities of the single-phase version and include new features that are not available in commercial meters. In fact, it is shown as the smart meter presented here is an alternative to commercial meters that, due to their high unit cost, cannot be deployed to multiple locations in electricity grids. Future work includes the design and implementation of a multi-phase version to be used by electrical machines of up to six phases.

Acknowledgments

This research has been supported by the Ministry of Science, Innovation and Universities at the University of Almeria under the programme "Proyectos de I+D de Generación de Conocimiento" of the national programme for the generation of scientific and technological knowledge and strengthening of the R+D+I system with grant number PGC2018-098813-B-C33.

References

[1] N. Uribe-Pérez, L. Hernández, D. De la Vega, I. Angulo, State of the art and trends review of smart metering in electricity grids, Applied Sciences 6 (3) (2016). doi:10.3390/app6030068.

[2] S. Kakran, S. Chanana, Smart operations of smart grids integrated with distributed generation: A review, Renewable and Sustainable Energy Reviews 81 (2018) 524–535. doi:https://doi.org/10.1016/j.rser.2017.07.045.

[3] A. Hirsch, Y. Parag, J. Guerrero, Microgrids: A review of technologies, key drivers, and outstanding issues, Renewable and Sustainable Energy Reviews 90 (2018) 402–411. doi:https://doi.org/10.1016/j.rser.2018.03.040.

[4] C. Chu, H. H. Iu, Complex networks theory for modern smart grid applications: A survey, IEEE Journal on Emerging and Selected Topics in Circuits and Systems 7 (2) (2017) 177–191. doi:10.1109/JETCAS.2017.2692243.

[5] Directive 2012/27/eu of the european parliament and of the council of 25 october 2012 on energy efficiency, amending directives 2009/125/ec and 2010/30/eu and repealing directives 2004/8/ec and 2006/32/ec text with eea relevance oj l 315, 14.11.2012, p. 1–56 (Oct 2012).
URL `https://eur-lex.europa.eu/eli/dir/2012/27/oj`

[6] M. H. Bollen, What is power quality?, Electric power systems research 66 (1) (2003) 5–14.

[7] J. Arrillaga, M. H. J. Bollen, N. R. Watson, Power quality following deregulation, Proceedings of the IEEE 88 (2) (2000) 246–261. doi:10.1109/5.824002.

[8] J. F. Fuller, E. F. Fuchs, D. J. Roesler, Influence of harmonics on power distribution system protection, IEEE Transactions on Power Delivery 3 (2) (1988) 549–557. doi:10.1109/61.4292.

[9] D. Sharon, J. Montano, A. Lopez, M. Castilla, D. Borras, J. Gutierrez, Power quality factor for networks supplying unbalanced nonlinear loads, IEEE Transactions on Instrumentation and Measurement 57 (6) (2008) 1268–1274. doi:10.1109/TIM.2007.915146.

[10] S. Khokhar, A. A. B. M. Zin, A. S. B. Mokhtar, M. Pesaran, A comprehensive overview on signal processing and artificial intelligence techniques applications in classification of power quality disturbances, Renewable and Sustainable Energy Reviews 51 (2015) 1650–1663. doi:10.1016/j.rser.2015.07.068.

[11] E. G. Ribeiro, T. M. Mendes, G. L. Dias, E. R. Faria, F. M. Viana, B. H. Barbosa, D. D. Ferreira, Real-time system for automatic detection and classification of single and multiple power quality disturbances, Measurement 128 (2018) 276–283. doi:https://doi.org/10.1016/j.measurement.2018.06.059.

[12] K. Sharma, L. Mohan Saini, Performance analysis of smart metering for smart grid: An overview, Renewable and Sustainable Energy Reviews 49 (2015) 720–735. doi:https://doi.org/10.1016/j.rser.2015.04.170.

[13] F. Alassery, Advanced metering infrastructure smart metering based on cloud architecture for low voltage distribution networks in application of smart grid monitoring, Sustainable Computing: Informatics and Systems 35 (2022) 100747. doi:10.1016/j.suscom.2022.100747.

[14] T.-C. Ou, C.-M. Hong, Dynamic operation and control of microgrid hybrid power systems, Energy 66 (2014) 314–323. doi:https://doi.org/10.1016/j.energy.2014.01.042.

[15] Y. H. Gu, M. H. J. Bollen, Time-frequency and time-scale domain analysis of voltage disturbances, IEEE Transactions on Power Delivery 15 (4) (2000) 1279–1284. doi:10.1109/61.891515.

[16] M. Uyar, S. Yildirim, M. T. Gencoglu, An expert system based on s-transform and neural network for automatic classification of power quality disturbances, Expert Systems with Applications 36 (3, Part 2) (2009) 5962–5975. doi:https://doi.org/10.1016/j.eswa.2008.07.030.

[17] R. G. Stockwell, L. Mansinha, R. P. Lowe, Localization of the complex spectrum: the s transform, IEEE Transactions on Signal Processing 44 (4) (1996) 998–1001. doi:10.1109/78.492555.

[18] M. Brenna, R. Faranda, E. Tironi, A new proposal for power quality and custom power improvement: Open upqc, IEEE Transactions on Power Delivery 24 (4) (2009) 2107–2116. doi:10.1109/TPWRD.2009.2028791.

[19] S. Dalai, B. Chatterjee, D. Dey, S. Chakravorti, K. Bhattacharya, Rough-set-based feature selection and classification for power quality sensing device employing correlation techniques, IEEE Sensors Journal 13 (2) (2013) 563–573. doi:10.1109/JSEN.2012.2219144.

[20] E. Viciana, A. Alcayde, F. G. Montoya, R. Baños, F. M. Arrabal-Campos, F. Manzano-Agugliaro, An open hardware design for internet of things power quality and energy saving solutions, Sensors 19 (3) (2019). doi:10.3390/s19030627.

[21] Electromagnetic compatibility (emc) - part 4-30: Testing and measurement techniques - power quality measurement methods, Tech. rep. (2015).

[22] En50160 voltage characteristics of electricity supplied by public distribution systems, Tech. rep., CENELEC (2010).

[23] F. G. Montoya, A. H. Eid, Formulating the geometric foundation of clarke, park, and fbd transformations by means of clifford's geometric algebra, Mathematical Methods in the Applied Sciences 45 (8) (2022) 4252–4277.

[24] J. Charras (Jan 2021). [link].
URL `https://kicad.org/`

[25] M. Frigo, S. G. Johnson, The design and implementation of fftw3, Proceedings of the IEEE 93 (2) (2005) 216–231. doi:10.1109/JPROC.2004.840301.

[26] L. D. O. Arenas, G. d. A. e Melo, C. A. Canesin, A methodology for power quantities calculation applied to an fpga-based smart-energy meter, IEEE Transactions on Instrumentation and Measurement 70 (2020) 1–11.

[27] Delorenzo loads for power electrical engineering, (Accessed on 2022-02-10).

URL https://bit.ly/3rSUm7a